Chiang Mai J. Sci. 2017; 44(3) : 1056-1064
http://epg.science.cmu.ac.th/ejournal/
Contributed Paper

Physicochemical Properties of Chromium-doped Titanium Dioxide Mesoporous and Its Application for Antifogging Materials

Hari Sutrisno* [a], Ariswan [b] and Dyah Purwaningsih [a]

[a] Department of Chemistry Education, Faculty of Mathematics and Natural Science, Yogyakarta State University, Kampus Karangmalang, Jl. Colombo No. 1, Yogyakarta, 55281, Indonesia.

[b] Department of Physic Education, Faculty of Mathematics and Natural Science, Yogyakarta State University, Kampus Karangmalang, Jl. Colombo No. 1, Yogyakarta, 55281, Indonesia.

* Author for correspondence; e-mail: sutrisnohari@uny.ac.id

Received: 28 September 2016
Accepted: 8 February 2017

ABSTRACT

Mesoporous materials of chromium doped titanium dioxide (Cr-doped TiO_2) and undoped TiO_2 were prepared by hot-injection reflux technique at 150 °C for 6 hours. Samples Cr-doped TiO_2 at different percentages: 1.1, 3.9 and 4.4 (wt% Cr) and undoped TiO_2 were synthesized from $Ti(O_2)O.2H_2O$ as titanium source obtained from the reaction of $TiCl_4$ and H_2O_2. Solid $(NH_4)_2CrO_4$ was a source of chromium as dopant. The prepared materials were characterized using powder X-ray diffraction (PXRD), scanning electron microscopy-energy dispersive X-ray spectroscopy (SEM-EDS) and N_2 adsorption-desorption isotherm. The XRD results reveal that the undoped TiO_2 is composed of well-crystalline anatase (major), rutile (minor) and brookite (minor) phases. In the 1.1.wt% Cr-doped TiO_2, its phase composition is anatase (major) and rutile (minor). The chromium dioxide (CrO_2), anatase (major), brookite and srilankite (TiO_2-II) are present in the 3.9 wt% Cr-doped TiO_2 and the 4.4 wt% Cr-doped TiO_2. All prepared materials (Cr-doped TiO_2 and undoped TiO_2) exhibit mesoporous of type-IV isotherm curves with H2-type hysteresis loop according to the IUPAC classication. The Brunauer-Emmett-Teller (BET) specific surface area (S_{BET}) and the mean pore size of the 4.4 wt% Cr-doped TiO_2 exhibit a maximum surface area of 111 m^2/g, corresponding to mean porous size of 4.95 nm. The hydrophilic properties of Cr-doped TiO_2 were investigated with illumination of UV light. All prepared samples shows excellent superhydrophilic properties. The 4.4 wt% Cr-doped TiO_2 demonstrates the most excellent superhydrophilic properties as compared with the other samples. These results allow the materials to be prospective application as antifogging.

Keywords: titanium dioxide, Cr-doped TiO_2, mesoporous, superhydrophilic, antifogging

1. INTRODUCTION

Among the various semiconductors, titanium dioxide (TiO_2) has been well known as an efficient phtocatalyst. This is because TiO_2 has the most efficient photoactivity, high refractive index, light absorption, non-toxicity, high chemical stability and relatively low-cost production [1]. When irradiated with ultraviolet or sun light on a TiO_2 surface, two phenomena of photochemical reaction will happen: the first is the photo-induced redox reactions, and the other is the photo-induced super-hydrophilic conversion. When the surface of TiO_2 was irradiated with light consisting of wavelengths shorter than its band gap, about 3.0-3.2 eV, electron and hole pairs are generated in the TiO_2, and they reduce and oxidize adsorbates on the surface, generating radical species such as $\times O_2$ and $\times OH$. Super-hydrophilic surfaces and reduction reactions at the surface of TiO_2 are a broad research field covering such as water cleaning [2], photo-electrochemical splitting of water [3], solar cells [4], self-cleaning [5], antifogging [6], anti-bacterial surface coatings [7], and photocatalyst [8]. Various applications of self-cleaning TiO_2 films have been proposed especially for practical applications such as window glasses, mirrors and windshields of automobile [9].

The performances and the properties of TiO_2 are strongly influenced by crystalline structure, morphology, surface states, size pore, dopant and size of the particles phase [10,11]. For TiO_2 photoinduced super-hydrophilicity, the main efforts have been made in two aspects: one is to narrow the wide bandgap to extend the spectral response of TiO_2 to the visible region for the efficient utilization of the energy from the sun. Another is to reduce the recombination rate of photogenerated electron-hole pairs to enhance efficiency of photolysis. Many efforts have been made to achieve the utilization of visible light for TiO_2 material, such as transitional metal ion doping [12, 13, 14], non-metal element doping [15, 16] and dye sensitization [17].

In the present study, a series various %wt Cr-doped TiO_2 and undoped TiO_2 have been successfully synthesized using a hot-injection reflux technique. The major goal were to synthesize and characterize undoped TiO_2 and a series various %wt chromium-doped TiO_2 and to investigate its photoinduced super-hydrophilic properties for antifogging materials.

2. MATERIALS AND METHODS

2.1 Materials

Ammonium hydroxide (NH_4OH, 28-30% NH_3) solution, hydrogen peroxide solution (H_2O_2, 10 wt% in H_2O), ammonium chromate $(NH_4)_2CrO_4$, 99%), titanium (IV) chloride ($TiCl_4$, 99%) were purchased from Sigma-Aldrich. All the reagents were used without further purification. Titanium dioxide hydrate was obtained from the reaction of $TiCl_4$ and H_2O_2 [18]. In a particular procedure, 15 ml $TiCl_4$ was added into a 500 ml glass flask loaded in an icewaterbath, then 30 ml of H_2O_2 was added slowly into the reaction vessel under magnetic stirring. The precipitate was filtered, washed with distilled water and dried at 100 °C for 5 hours.

2.2 Sample Preparation

A series of chromium doped TiO_2 at various %wt Cr were prepared by a reflux technique. In a particular procedure, 10 g of titanium dioxide hydrate was dissolved in 50 ml of distilled water under vigorous stirring and was stirred for 4 hours to obtain colloid labeled P. For studying the effect of the $(NH_4)_2CrO_4$ concentration, in a separated beaker 0, 3, 6 and 9 wt% Cr-doped TiO_2 respectively were adopted. It was

dissolved in 20 mL of distilled water thoroughly under vigorous stirring to obtain solutions labeled Q_1, Q_2, Q_3, and Q_4 respectively. Each solution Q_1, Q_2, Q_3, and Q_4 was then slowly added to each solution P. The solution mixture was heated at 150 °C with a magnetic stirrer in equipment reflux, added dropwise NH_4OH until pH to about 8-10 within about 10 minutes. The solution mixture was refluxed at 150 °C for 6 hours. The precipitate was filtered, washed with distilled water and dried at 70 °C for 3 hours. Furthermore, the precipitate was calcined at 600 °C for 2 hours.

2.3 Physical Measurements of Samples

The morphologies of the prepared materials were observed by a scanning electron microscope (Phenom ProX Desktop SEM) equipped energy dispersive X-ray spectroscopy (EDS). Sample surface was observed and the images were recorded. EDS was used to analyze the presence of Ti, and O elements in the TiO_2 and the presence of Ti, Cr, and O elements in the Cr-doped TiO_2.

The powder XRD patterns of prepared materials were collected using a Rigaku Miniflex 600-Benchtop X-ray diffractometer, operating in the Bragg configuration using Cu Kα radiation (λ = 1.5406 Å) at a tube current of 15 mA and a voltage of 40 kV. Data were collected over 2q values from 2 - 90°. The measurements were recorded in steps of 0.02° with a count time of 5 s/step at room temperature 25 °C. The qualitative analysis was carried out with the identification of a phase or phases in the samples by comparison with "standard" patterns: COD and ICDD. The average crystallite size of anatase and rutile were calculated based on XRD peak broadening using the basic Scherrer formula (Eq. (1)) [19], which is then modified and written as Eq. (2). It is modified by making logarithm on both sides:

$$\beta = \frac{K\lambda}{Lcos\theta} = \frac{K\lambda}{L} - \frac{1}{cos\theta} \quad \text{..... (1)}$$

$$\ln\beta = \ln\frac{K\lambda}{Lcos\theta} = \ln\frac{K\lambda}{L} + \ln\frac{1}{cos\theta} \quad \text{..... (2)}$$

where L is the average crystallite size, β is the peak width of the diffraction peak profile at half maximum height (FWHM) resulting from small crystallite size in radians and K is a constant related to crystallite shape, normally taken as 0.9, l is the wavelength of the X-ray radiation (λ K_α(Cu) = 1.5406 nm) and θ is the Bragg angle. If we plot the results of ln β against ln (1/cos qθ, then a straight line with a slope of around one and then an intercept of about ln K/L must be obtained. The mean crystallite size of anatase particle was estimated by analysing the broadening of the (101), (004), (200), (211), and (220), reflections. While the mean crystallite size of rutile particle was estimated by analysing the broadening of the (110), (101), (111), (210), and (220), reflections. The average crystallite size of brookite and srilankite (TiO_2-II) were calculated based on XRD peak broadening using the Scherrer Formula (Eq.(1)).

Full adsorption-desorption isotherms data of nitrogen at 77 K on all prepared materials were collected at various partical pressures in a Surface Area and Pore Porosimetry Analyzer ASAP 2020 instrument from Micromeritics. Before the BET/BJH measurements, the prepared materials were degassed at 150 °C under vacuum for 4 h prior to analysis with a vacuum set point of 10 mmHg. The Brunauer-Emmett-Teller (BET) specific surface data area (S_{BET}) was determined by a multipoint BET method using the adsorption data in the relative pressure ($P/P0$) of ~ 0.30 [20]. The pore size distribution was evaluated from the adsorption-desorption branch of the

isotherms by the procedure developed by Barrett, Joyner and Halenda (BJH) [21]. The nitrogen adsorption and desorption volume at the relative pressure ($P/P0$) of ~ 0.99 was used to determine the pore volume and the average pore size.

2.4 Study of Photoinduced Superhydrophilic Properties

Ultraviolet-ray irradiated to the surface of the prepared sample by commercial 20W black light blue fluorescent light, and the contact angle of water was measured every 2 minute.

3. RESULTS AND DISCUSSIONS

3.1 Scanning Electron Microscopy (SEM)

Figure 1 show typical SEM images and EDS analysis of TiO_2 and Cr-doped TiO_2 nanoparticles.

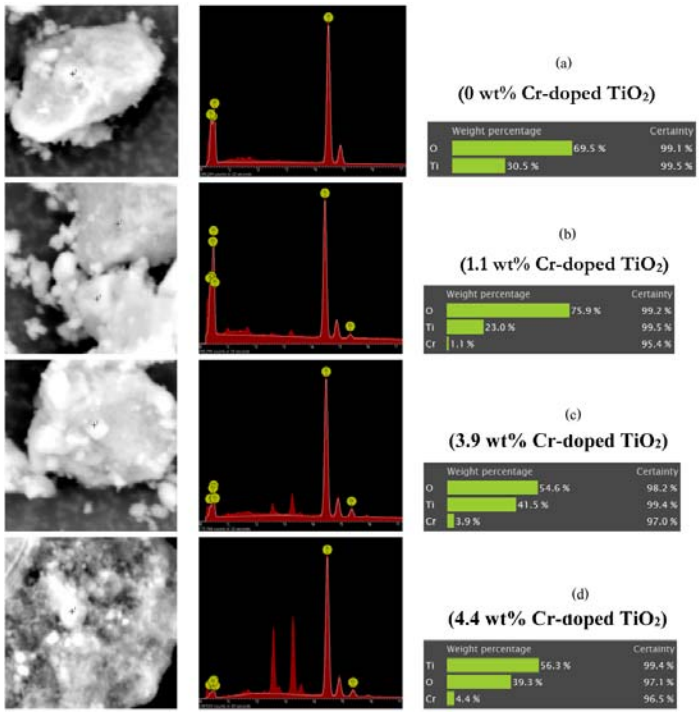

Figure 1. SEM image (left), EDS analysis (middle) and weight percentage of Ti, O and Cr in the prepared samples (right): (a) undoped TiO_2, (b) 1.1 wt% Cr-doped TiO_2, (c) 3.9 wt% Cr-doped TiO_2, and (d) 4.4 wt% Cr-doped TiO_2.

SEM micrographs and EDS spectra of TiO_2 (Figure 1(a)) and 1.1., 3.9, and 4.4 wt% Cr-doped TiO_2 (Figure 1(b-d)) prepared by reflux technique show the formation of aggregated secondary particles by the agglomeration of primary particles. On the theoretical basis, addition of each: 3, 6 and 9 wt% Cr-doped TiO_2 should produce experimentally only 1.1, 3.9 and 4.4 wt% Cr-doped TiO_2, respectively. The EDS analysis reveals the presence of Ti and O elements in TiO_2 and the presence of Ti, Cr and O elements in various wt% Cr-doped TiO_2.

3.2 X-ray Diffraction (XRD)

Figure 2 represents the XRD patterns of undoped TiO_2 and Cr-doped TiO_2.

The undoped TiO_2 shows that anatase (major), rutile (minor) and brookite (minor) forms are obtained by reflux technique.

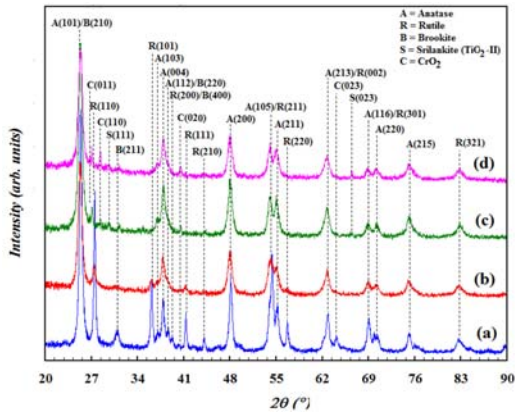

Figure 2. PXRD pattern of the prepared samples: (a). undoped TiO_2, (b). 1.1 wt% Cr-doped TiO_2, (c). 3.9 wt% Cr-doped TiO_2, and (d). 4.4 wt% Cr-doped TiO_2.

From the XRD pattern (Figure 2(a)), the peak position at 2q = 25.36□, 37.84□, 48.11□, 54.38□, 55.07□, and 62.88□ are indexed as the (101), (103), (200), (105), (211), and (213) reflections of crystalline anatase phase, corresponding to those shown in the ICDD card No. 00-021-1272. The other diffraction peaks are observed 2q = 27.53□, 36.14□, 39.24□, 41.32□, and 54.38□ are indexed as the (110), (101), (200), (111), and (211) reflections of crystalline rutile phase, corresponding to those shown in the COD card No. 9004141. The three distinct diffraction peaks are clearly observed at 2q = 25.36□, 30.95□, and 39.24□ being assigned to (210), (211), and (400) reflections of brookite phase, respectively, corresponding to those shown in the ICDD card No. 00-016-0617. In the 1.1.wt% Cr-doped TiO_2, its phase composition are anatase (major) and rutile (minor). The chromium oxide (CrO_2), anatase (major), brookite and srilankite (TiO_2-II) are present in the 3.9 wt% Cr-doped TiO_2 and the 4.4 wt% Cr-doped TiO_2.

The phase composition, the average crystallite sizes (*L*) of the phases in undoped TiO_2 and Cr-doped TiO_2 are given in Table 1. It is clear that the crystallite size of anatase decreases (114.09-110.17 nm) with increasing the molar of doping agent (Cr). The crystallite size of anatase and rutile increase with the presence of doping agent (Cr).

3.3 N_2 Adsorption-Desorption Isotherm

To investigate the pore size distribution and adsorption properties of undoped TiO_2 and various wt% Cr-doped TiO_2, N_2 adsorption-desorption isothermal tests were carried out using BET-BJH method, and their isotherm curves were presented in Figure 3. In all prepared materials, it can be observed that the powder exhibits the classical shape of type-IV isotherm curves with H2-type hysteresis loop according to the IUPAC classication [22, 23]. Their narrow hysteresis loops exhibit a typical pattern of Type IV at a relative pressure from 0.68 to 0.98 (undoped TiO_2), 0.60 to 0.92 (1.1 wt% Cr-doped TiO_2), 0.42 to 0.92 (3.3 wt% Cr-doped TiO_2) and 0.45 to 0.90 (4.4 wt% Cr-doped TiO_2), indicating that the prepared materials have characteristic of a material that contains mesoporosity and has a high energy of adsorption. In addition, the hysteresis loops for these materials are H2 which means that the material is often associated pores with narrow and wide sections and possible interconnecting channels.

The pore size distribution of undoped TiO_2 and various wt% Cr-doped TiO_2 depicted in Figure 4 (inset) show a porosity in the range of 4.95-12.16 nm. The surface area, volume and pore size distribution of the prepared materials (Cr-doped TiO_2 and undoped TiO_2) have been summarized in Table 2.

Table 1. Phase and crystallite size of undoped TiO_2 and Cr-doped TiO_2.

Sample	Phase*)	Hkl	2θ (°)	d (Å)	FWHM 2θ (deg)	L **) (nm)
Undoped TiO_2	Anatase	(101)	25.36	3.509	0.42	193.84
		(004)	37.84	2.376	0.43	
		(200)	48.11	1.889	0.47	
		(211)	55.07	1.666	0.47	
		(220)	70.34	1.337	0.50	
	Rutile	(110)	27.53	3.237	0.25	323.83
		(101)	36.14	2.483	0.29	
		(111)	41.32	2.183	0.24	
		(210)	44.13	2.050	0.26	
		(220)	56.63	1.624	0.29	
	Brookite	(211)	30.95	2.887	0.67	122.99
1.1 wt% Cr-doped TiO_2	Anatase	(101)	25.29	3.519	0.72	114.09
		(004)	37.75	2.381	0.74	
		(200)	48.00	1.894	0.70	
		(211)	55.12	1.665	0.49	
		(220)	70.18	1.340	0.86	
	Rutile	(110)	27.45	3.247	0.47	178.04
		(101)	36.05	2.489	0.52	
3.9 wt% Cr-doped TiO_2	Anatase	(111)	41.24	2.187	0.51	110.17
		(101)	25.31	3.516	0.73	
		(004)	37.92	2.371	0.76	
		(200)	48.01	1.894	0.77	
		(211)	55.03	1.667	0.79	
		(220)	70.15	1.341	0.84	
	Brookite	(211)	31.13	2.870	0.28	294.42
	CrO_2	(011)	27.11	3.287	0.18	572.86
		(110)	28.40	3.139	0.10	
		(020)	40.56	2.222	0.19	
	TiO_2-II	(111)	29.62	3.013	0.44	186.69
4.4 wt% Cr-doped TiO_2	Anatase	(101)	25.33	3.513	0.72	112.59
		(004)	37.83	2.377	0.74	
		(200)	48.01	1.894	0.76	
		(211)	55.06	1.667	0.80	
		(220)	70.11	1.341	0.84	
	Brookite	(211)	31.29	2.8567	0.12	687.24
	CrO_2	(011)	27.06	3.292	0.11	506.69
		(110)	28.39	3.141	0.20	
		(020)	40.43	2.229	0.23	
	TiO_2-II	(111)	29.53	3.022	0.39	210.58

*) The phase composition was determined by qualitative analysis ("standard" patterns: COD and ICDD)

**) The average crystallite size of anatse and rutile were calculated by Modified Debye-Scherrer formula, while for CrO_2, brookite and srilankite were calculated by Debye-Scherrer formula

Table 2. Surface area, volume and pore size distribution of Cr-doped TiO_2 and undoped TiO_2 from Nitrogen Adsorption-desorption Isotherm Measurements.

Sample	Surface Area BET (S_{BET}) (m^2/g)	Pore Volume at $P/P_o \approx 0.99$ (cm^3/g)	Pore Size (nm)
Undoped TiO_2	33	0.1168	12.16
1.1 wt% Cr-doped TiO_2	65	0.1658	8.01
3.9 wt% Cr-doped TiO_2	30	0.0591	6.88
4.4 wt% Cr-doped TiO_2	111	0.1612	4.95

The BET surface area and the mean pore size of the 4.4 wt% Cr-doped TiO_2 exhibit a maximum surface area of 111 m^2/g, corresponding to mean porous size of 4.95 nm. The pore size distribution curve calculated from the desorption branch of the isotherm BJH analyses shows that the undoped TiO_2 exhibits pore size of 12.16 nm and the 1.1, 3.9, and 4.4 wt% Cr-doped TiO_2) exhibit pore sizes of 8.01, 6.88, and 4.95 nm (inset Figure 3), respectively.

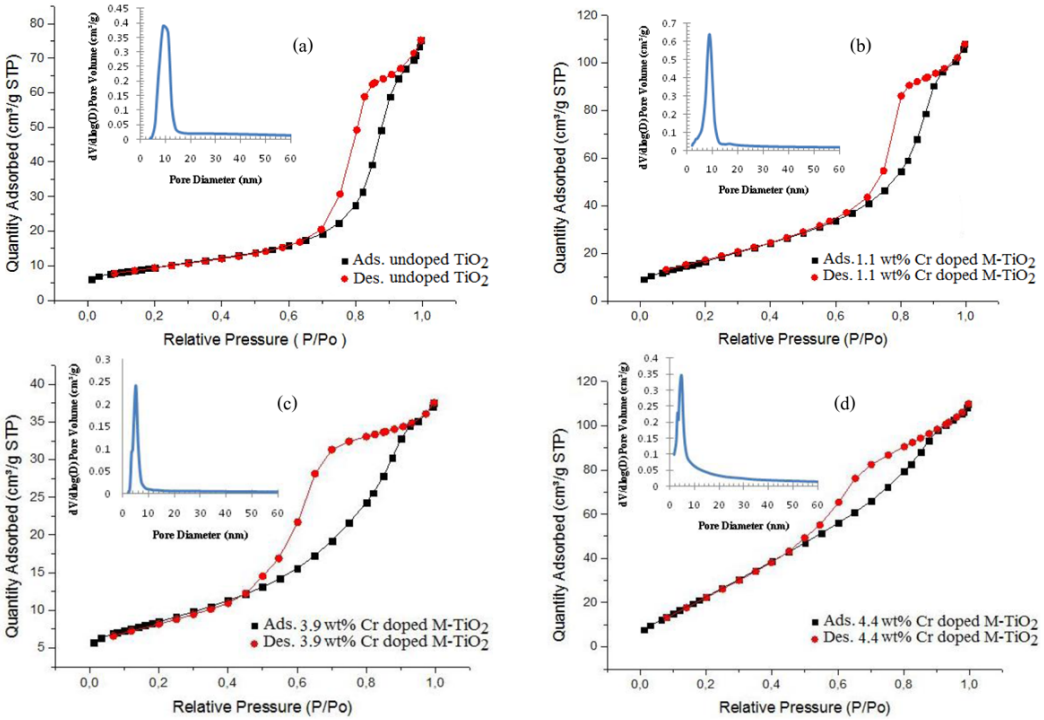

Figure 3. Nitrogen adsorption-desorption isotherms of the prepared samples: (a) undoped TiO_2, (b) 1.1 wt% Cr-doped TiO_2, (c) 3.9 wt% Cr-doped TiO_2, and (d) 4.4 wt% Cr-doped TiO_2 (inset of pore size distribution from the adsorption branch of isotherm).

3.4 The Contact Angle Changes of Water on the Cr-doped TiO_2 Surface Irradiated by Ultra-Violet (UV) Light

Figure 4 shows diagram of the change of contact angles of water dropped on the UV-iradiated undoped TiO_2 and Cr doped TiO_2 films. The contact angle of water on the prepared samples surfaces can be altered by UV irradiation.

From the diagram in Figure 4, it can be seen that the 4.4 wt% Cr-doped TiO_2 has the most excellent superhydrophilic properties as compared with other samples. The phenomena after UV irradiation for 40 minutes are as follows:

-Undoped TiO_2, irradiation with UV light inducing a decrease in contact angle from about 46.93° to 25.51°.

- 1.1 wt% Cr-doped TiO_2, irradiation with UV light inducing a decrease in contact angle from about 46.48° to 24.52°.

- 3.9 wt% Cr-doped TiO_2, irradiation with UV light inducing a decrease in contact angle from about 44.84° to 22.38°.

- 4.4 wt% Cr-doped TiO_2, irradiation with UV light inducing a decrease in contact angle from about 46.12° to 19.04°.

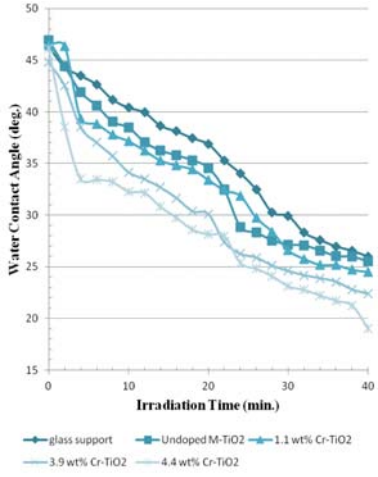

Figure 4. Change of the contact angles for film of glass support, undoped TiO_2, 1.1 wt% Cr-doped TiO_2, 3.9 wt% Cr-doped TiO_2, and 4.4 wt% Cr-doped TiO_2 with UV irradiation.

4. CONCLUSIONS

A various wt% chromium-doped TiO_2 (Cr-doped TiO_2) and undoped TiO_2 have been successfully synthesized by hot-injection reflux technique. The prepared samples consist of anatase (major), rutile (minor), chromium oxide (CrO_2) (minor), brookite (minor) and srilankite (TiO_2-II) (minor) type structures. In the 1.1.wt% Cr-doped TiO_2, its phase composition is anatase (major) and rutile (minor). The CrO_2, anatase, brookite and srilankite (TiO_2-II) are present in the 3.9 wt% Cr-doped TiO_2 and the 4.4 wt% Cr-doped TiO_2. The BET surface area and the mean pore size of the 4.4 wt% Cr-doped TiO_2 exhibit a maximum surface area of 111 m^2/g, corresponding to mean porous size of 4.95 nm. All prepared materials (Cr-doped TiO_2 and undoped TiO_2) exhibit mesoporous of type-IV isotherm curves with H2-type hysteresis loop according to the IUPAC classication. The hydrophilic properties of Cr-doped TiO_2 were investigated with illumination of UV light, and all prepared samples show excellent super-hydrophilic properties, and the 4.4 wt% Cr-doped TiO_2 exhibits the most excellent superhydrophilic properties as compared with other samples. These results allow the materials to be prospective application as antifogging.

ACKNOWLEDGEMENTS

This work was financially supported by the Directorate General of Higher Education - Ministry of Education and Culture of the Republic of Indonesia based on PUPT 2014 Grant, No. 230/UPT-BOPTN/UN34.21/2014.

REFERENCES

[1] Carp O., Huisman C.L. and Reller A., *Prog. Solid State Chem.*, 2004; **32**: 33-177. DOI10.1016/j.progsolidstchem.2004.08.001.

[2] Dai Q., Zhang Z., He N., Li P. and Yuan C., *Mater. Sci. Eng.,* 1999; **C8-9**: 417-423. DOI 10.1016/S0928-4931(99)00016-8.

[3] Huang C.W., Liao C.H. and Wu J.C.S., *J. Clean Energy Technol.,* 2013; **1(1)**: 1-5. DOI 10.7763/JOCET.2013.V1.1.

[4] Dwivedi C., Dutta V., Chandiran A.K., Nazeeruddin M.K. and Gratzel M., *Energy Procedia*, 2013; **33**: 223-227. DOI 10.1016/j.egypro.2013.05.061.

[5] Lopes de Jesus M.A.M, Trajano da Silva Neto J., Timó G., Paiva P.R.P., Dantas M.S.S. and Mello Ferreira A., *Appl. Adhes. Sci.*, 2015; **3(5)**: 2-9. DOI 10.1186/s40563-015-0034-4.

[6] Lai Y., Tang Y., Gong J., Gong D., Chi L., Changjian Lin C. and Chen Z., *J. Mater. Chem.*, 2012; **22**: 7420-7426. DOI 10.1039/C2JM16298A.

[7] Kong H., Song J. and Jang J., *Environ. Sci. Technol.*, 2010, **44(14)**: 5672-5676. DOI 10.1021/es1010779.

[8] Chen F., Zou W., Qu W., and Zhang J., *Catal. Commun.*, 2009; **10**: 1510-1513. DOI 10.1016/j.catcom.2009.04.005.

[9] Worasukhkhung S., Pudwat S., Eiamchai P., Horprathum M., Dumrongrattana S. and Aiempanakit K., *Proc. Eng.*, 2012; **32**: 780-786. DOI 10.1016/j.proeng.2012.02.012.

[10] Masuda Y. and Kato K., *Chem. Mater.,* 2008; **20**: 1057-1063. DOI 10.1021/cm071026t.

[11] Testino A., Bellobono I.R., Buscaglia V., Canevali C., D'Arienzo M., Polizzi S., Scotti R. and Morazzoni F., *J. Am. Chem. Soc.*, 2007; **129(12)**: 3564-3575. DOI 10.1021/ja067050+.

[12] Li Z., Ding D. and Ning C., *Nanoscale Res. Lett.*, 2013; **8(25)**: 1-8. DOI 10.1186/1556-276X-8-25.

[13] Tian B., Li C. and Zhang J., *Chem. Eng. J.*, 2012; **191**: 402-409. DOI 10.1016/j.cej.2012.03.038.

[14] Thuy N.M., Van D.Q. and Hai L.T.H., *Nanomater. Nanotechnol.*, 2012; **2(14)**: 1-8. http://hrcak.srce.hr/file/210797.

[15] Nishikiori H., Hayashibe M. and Fujii T., *Catalysts*, 2013; **3**: 363-377. DOI 10.3390/catal3020363.

[16] Yang G., Jiang Z., Shi H., Xiao T. and Yan Z., *J. Mater. Chem.*, 2010; **20**: 5301-5309. DOI 10.1039/C0JM00376J.

[17] Gr□tzel M., *Inorg. Chem.*, 2005; **44**: 6841-6851. DOI 10.1021/ic0508371

[18] Rich R.L., *Inorganic Reactions in Water*, Springer, 2006.

[19] Monshi A., Foroughi M.R., and Monshi M.R., *World J. Nano Sci. Eng.*, 2012; **2**: 154-160. DOI 10.4236/wjnse.2012.23020.

[20] Brunauer S., Emmett P.H. and Teller E., *J. Am. Chem. Soc.*, 1938; **60(2)**: 309-319. DOI 10.1021/ja01269a023.

[21] Barrett E.P., Joyner L.G. and Halenda P.P., *J. Am. Chem. Soc.*, 1951; **3(1)**: 373-380. DOI 10.1021/ja01145a126.

[22] Lowell S., Shields J.E., Thomas M.A. and Thommes M., *Characterization of Porous Solids and Powders: Surface Area. Pore Size and Density*, Springer, 2006,

[23] Condon J.B., *Surface Area and Porosity Determinations by Physisorption Measurements and Theory*, Elsevier, 2006.